Received: 28 January 2023 | Accepted: 27 July 2023

DOI: 10.1111/aos.15744

Acta Ophthalmologica

ORIGINAL ARTICLE

Non-invasive biomarkers for close activity monitoring in birdshot chorioretinitis: Optical coherence tomography angiography and beyond

Aina Moll-Udina[1,2] | Marina Dotti-Boada[1] | Lucía Miguel[1,2] | Anabel Rodríguez[1] | Jesús Gascón[1] | Maite Sainz de la Maza[1,2] | Alfredo Manuel Adán Civera[1,2] | Blanca Molins[2] | Victor Llorenç[1,2]

[1]Clinic Institute of Ophthalmology (ICOF), Clinic Hospital of Barcelona, Barcelona, Spain

[2]August Pi i Sunyer Biomedical Research Institute (IDIBAPS), Barcelona, Spain

Correspondence
Aina Moll-Udina, Clinic Institute of Ophthalmology (ICOF), Clínic Hospital of Barcelona, Sabino de Arana 1, Barcelona 08028, Spain.
Email: moll@clinic.cat

Abstract

Purpose: The purpose of the study was to identify non-invasive imaging biomarkers potentially useful for close activity monitoring in birdshot chorioretinitis (BSCR).

Methods: Cross-sectional study of BSCR eyes included as per Levinson's and/or SUN criteria. Eyes were blindly classified into active or inactive groups per clinical inflammatory parameters, ultra-widefield (UWF) pseudocolour images, UWF fluorescein angiography (FA) and macular optical coherence tomography (OCT) cube. Qualitative and quantitative OCT and OCT-angiography (OCT-A) parameters at the fundus, superonasal and inferonasal fields were compared between active and inactive eyes.

Results: Thirty consecutive BSCR patients (60 eyes) were analysed. 28 eyes (46.66%) were from women and the overall mean age was 59.7 ± 12.3 years. Active eyes showed an abnormal retinal thickening at inferonasal field (nasal retinal thickness) and a higher averaged thickened retinal index (ATRI) (72.36 active vs. 20.12 inactive, $p<0.0001$). A significant moderate correlation was observed between ATRI and FA scores ($r=0.259$, $p=0.022$). Macular vascular loops were more frequent in the superficial vascular plexus of OCT-A in the active eyes ($p=0.028$). The vascular perfusion index tended to be higher in all subfields of active eyes but did not reach statistical significance.

Conclusion: Multimodal imaging could be key to discerning activity in BSCR eyes. Higher ATRI and the presence of vascular loops in the superficial plexus are potential non-invasive activity biomarkers for the close monitoring of BSCR.

KEYWORDS

biomarkers, birdshot, ocular inflammation, optical coherence tomography, optical coherence tomography angiography, uveitis

1 | INTRODUCTION

Birdshot chorioretinitis (BSCR) is a bilateral, chronic posterior non-infectious uveitis that preferentially affects middle-aged Caucasians. It is characterized by distinctive multiple hypopigmented retinochoroidal lesions in combination with retinal vasculitis and mild vitritis (Monnet et al., 2006). These BSCR spots are predominantly located on the posterior pole, radiating from the optic nerve to the mid-peripheral retina, typically, to the inferonasal field (Levinson et al., 2006). It is an eye-restrictive disease with no predominant extraocular manifestation associated (Bousquet et al., 2022; Pagnoux et al., 2010). BSCR incidence is estimated at 0.6%–1.5% in uveitis patients and 6%–8% in patients with posterior uveitis (Shah et al., 2005).

In 2021, the SUN working group described BSCR classification criteria for use in clinical practice and research. Among others, key features included bilateral hypofluorescent dark dots in the indocyanine green

angiogram (ICGA), without BSCR spots upon ophthalmoscopy (SUN, 2021). Early diagnosis and the instauration of appropriate treatment are probably key in preventing the cumulative damage caused by chronic inflammation. Thus, early clinical suspicion via ICGA in non-spotted eyes could be crucial (Cao et al., 2016; Knecht et al., 2014).

BSCR is a T-cell-mediated uveitis where the HLA-A*29:02 haplotype and certain endoplasmic reticulum aminopeptidase (ERAP) variants are strongly related to BSCR physiopathology (Fich & Rosenberg, 1992; Kuiper et al., 2014; Nussenblatt et al., 1982).

Given the slow, progressive nature of the disease, careful monitoring to measure accumulated retinal damage over the years is essential. Classic BSCR monitoring is performed by studying the visual field (VF) (Arya et al., 2015; Thorne et al., 2008) and electroretinogram (ERG) (Sobrin et al., 2005; Zacks et al., 2002). The visual field usually requires a 30–2 (peripheral) strategy to pick up early changes; moreover, small changes are hard to interpret in eyes with low contrast sensitivity and other qualitative visual disabilities, such as in BSCR. ERG is an invasive time-consuming test that cannot be conducted frequently, limiting the appropriate close follow-up that many early BSCR patients require. Therefore, while the 30–2 visual field and ERG have classically been key tests to monitor BSCR progression in the long term, their sensitivity and feasibility to detect treatable activity in daily practice are limited (Böni et al., 2017). On the other hand, classic 7- to 9-field fluorescent angiography (FA) is an incomplete invasive test proposed to monitor BSCR inflammatory retinal activity. Ideally, it should be combined with ICGA to monitor stromal choroidal inflammation in a dual manner (Tugal-Tutkun et al., 2010). Therefore, BSCR closely monitored via angiography could harbour ethical concerns, including patient discomfort, being time-consuming and expensive procedures.

In summary, multimodal imaging including FA, ICGA, fundus autofluorescence (FAF) and structural optical coherence tomography (OCT) have been described as helpful in BSCR diagnosis, prognosis and for monitoring disease activity, however, to discern disease activity and progression in the short term remains still challenging (Bousquet et al., 2022; Pohlmann et al., 2017). Fundus autofluorescence and OCT can reveal ellipsoid zone disruption in BSCR, nevertheless, it is considered a sign of structural damage, rather than an activity sign (Teussink et al., 2016).

Currently, new qualitative and quantitative parameters assessed via multimodal imaging techniques can delve deeper into the inflammation and progression of the disease (Pohlmann et al., 2017). Ultra-widefield (UWF) imaging, high-resolution *en face* retinal colour maps on OCT and, more recently, OCT-angiography (OCT-A) are new sources of potential sensitive and feasible non-invasive biomarkers that might help in the frequent monitoring of diseases with otherwise limited and low-sensitivity options, such as BSCR.

This study aimed to determine potential non-invasive activity biomarkers of BSCR by multimodal imaging, assessing qualitative and quantitative differences in retinal and choroidal anatomy and microvasculature, both in macular and extramacular areas at the nasal subfields.

2 | MATERIALS AND METHODS

This was a cross-sectional study of consecutive BSCR cases from December 2018 to December 2022 in a tertiary uveitis clinic (Clínic Hospital of Barcelona, Spain).

Inclusion criteria were patients with BSCR diagnosed by Levinson and/or SUN criteria (Levinson et al., 2006; SUN, 2021). Exclusion criteria were corneal or lens opacities that precluded visualization of the fundus or prevented good OCT imaging and concurrent chorioretinal diseases that interfered with proper BSCR assessment.

Demographic and clinical data were collected at inclusion. To conduct this study, the eyes included were divided into two groups (active and inactive) by two independent uveitis senior specialists and in the case of discrepancies, a consensus on the activity/inactivity status was discussed and finally assigned to one group (A.A., M.S. and V.L.).

Classification criteria of active or inactive group were done by (1) Clinical assessment: slit lamp examination, including anterior chamber cell grading (ACC, SUN scale) (Jabs et al., 2005) and indirect ophthalmoscopy, including vitreous haze grading (VH, NEI scale) (Nussenblatt et al., 1985); (2) Fundus features (pigmentation, number, location and size of BSCR spots) were performed via the Optos UWF fundus pseudocolour imaging system (OptosPLC, Dunfermline, UK); (3) UWF fluorescein angiography (FA), scored according to the Angiography Scoring for Uveitis Working Group (ASUWOG) (Tugal-Tutkun et al., 2010). Due to the lack of healthcare authority approval for indocyanine green use in humans, UWF-ICGA could only be performed off-label in selected patients with doubtful disease activity; (4) OCT scans (spectral-domain [SD] OCT; Cirrus HD-OCT®, Carl Zeiss Meditec) were obtained for all eyes after pupillary dilation at the fundus field, centred on the fovea (Macular cube 512 × 128 μm within a 6 × 6 mm area), to measure the central macular thickness (CMT) and macular volume.

The study protocol was performed in three different retinal fields: fundus field, superonasal field and inferonasal field, taking the foveola and optic disc edge as a reference, respectively. Nasal retinal thickness and nasal volume were automatically determined by the manufacturer's built-on software, as quantitative data in the inferonasal field.

The enhanced deep imaging (EDI) protocol was employed for the assessment of choroidal thickness and qualitative data, recorded as per the presence of cystic spaces, epiretinal membrane and ellipsoid layer integrity (normal, damaged or absent) in the fundus field and inferonasal Field.

OCT-angiography (Angioplex®, Carl Zeiss Meditec) 6 × 6 and 3 × 3 mm retinal vasculature analysis was performed by automated segmentation of the superficial capillary plexus. Retinal vascular density (VD) and perfusion index (PI) were automatically determined by the Angioplex® interface with an ETDRS grid in the

superficial capillary plexus of the fundus, superonasal and inferonasal fields. The area, perimeter and circularity of the foveal avascular zone (FAZ), as well as the qualitative assessment of the superficial capillary plexus were studied with a 3 × 3 mm Angioplex® frame (fundus field). We recorded the presence of telangiectasias, increased intercapillary spaces, capillary irregularity and capillary loops. Figure 1 shows the OCT and OCT-A image acquisition protocols at different retinal fields.

OCT-A all retina *en face* thickness maps of the fundus field were exported in colour scale for processing and calculating the averaged index of the amount of red and blue in RGB (Red-Green-Blue) units per area in pixels. The averaged thickened retinal index (ATRI) and the averaged atrophy retinal index (AARI) were studied after thickness map processing, as described elsewhere (Llorenç et al., 2021).

The study protocol was approved by the Ethics Committee of the Clinic Hospital of Barcelona (HCB/2020/0472), which followed the tenets of the Declaration of Helsinki (October 2013) and all patients provided written informed consent.

Statistical analysis. Categorical variables were expressed as absolute numbers and percentages. Fisher's exact test or Kruskal–Wallis test were used to compare categorical variables with two or more categories. Continuous variables were expressed as mean and standard deviation or median and interquartile range. The Mann–Whitney *U*-test was used to compare continuous variables between the active and inactive groups. Spearman's coefficient was used to search for correlational relationships between variables. For a multivariate approach, due to the high collinearity among covariates, a partial least square discriminant analysis (PLS-DA) between active and inactive eyes was implemented. Covariates with $p \leq 0.01$ in the univariate analysis or those clinically meaningful (age, evolution time to baseline, sex) were included in the model. A threshold of less than 5% in the alpha error was set as statistically significant.

3 | RESULTS

Regarding demographics, 32 HLA-A*29 positive Caucasian patients were included, totalling 64 eyes. Classification agreement was reached in 57/64 eyes (89%), whereas 7 eyes showed discrepancies, and were finally classified after discussion with a third uveitis specialist. Figure 2 shows an example of an active and inactive patients as classification criteria. Four eyes from two patients were excluded due to concurrent chorioretinal comorbidity, one with myopia magna and the other with a macular neovascular membrane in one eye and macular scarring in the other; therefore, 60 eyes from 30 patients were finally analysed. Eight patients were in both groups with one active and one inactive fellow eye, as per uveitis expert consensus. 28 eyes (46.66%) were from women, and patients had an overall mean age of 59.7 ± 12.3 years and a mean evolution time until inclusion of 111 ± 67.9 months. No statistically significant differences were found between active and inactive groups for these variables.

Visual fields were not performed at the cut point of this study. However, when the nearest visual fields to the cut point were studied, they showed abnormalities in 89% and 92% of active and inactive eyes, respectively. Surprisingly, no significant differences in the mean deviation (MD) were observed between both groups (MD, dB; mean ± SD, active = −11.11 ± 10.6 dB vs. inactive = −15.8 ± 9 dB; $p = 0.132$).

As expected, eyes classified as active showed higher vitreous haze and angiography scores, a moderate number of medium-sized spots (4–20 spots), as well as higher macular thickness and volume, as compared to inactive eyes (Table 1).

Regarding SD-OCT quantitative structural assessment, nasal retinal thickness was significantly greater in the active group: 236.27 versus 207.27 μm for inactive ($p < 0.0001$) at the inferonasal field (Figure 3d).

Macular high-definition raster B-scans showed that epiretinal membranes ($p = 0.043$) and a trend towards better ellipsoid layer integrity ($p = 0.066$) were more frequent in active eyes compared with inactive. Interestingly, although thicker in the active group, choroidal thickness was not significantly higher compared with the inactive group in any studied subfield.

Processing and quantification of high-resolution colour all retina thickness maps showed a significantly higher ATRI in the active group (72.36 vs. 20.12, $p < 0.0001$), whereas AARI was significantly lower compared with the inactive group (67.15 vs. 137.89, $p < 0.0001$). (Table 2; Figure 3a,b).

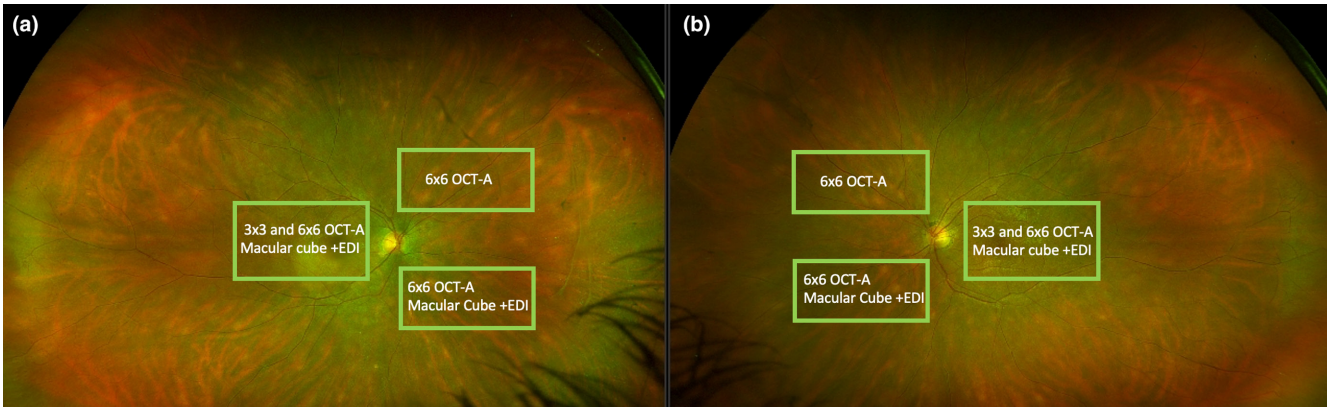

FIGURE 1 Image acquisition protocols in right and left eye (a, b) of a BSCR patient.

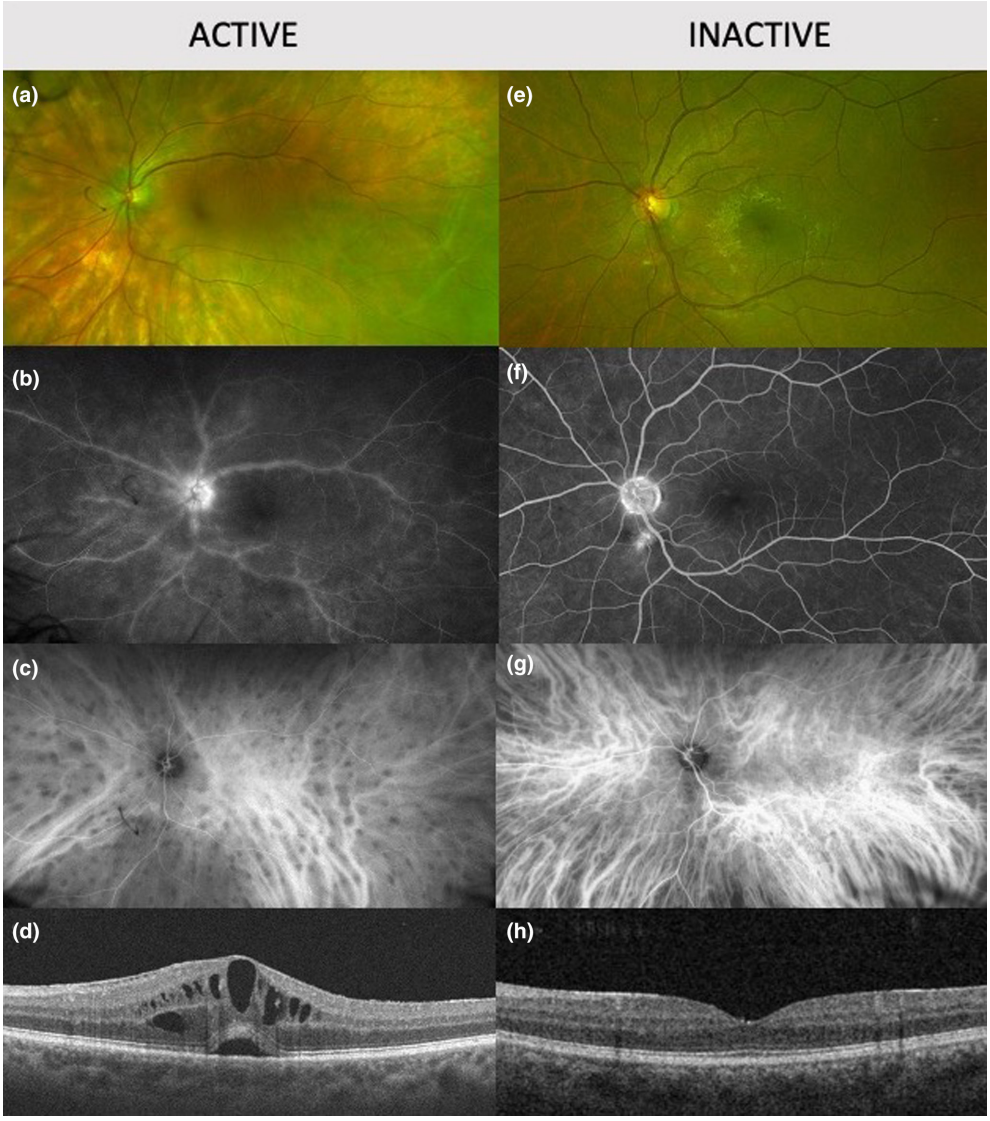

FIGURE 2 Active (left column) and inactive (right column) BSCR patients as classification criteria. (a) Optos UWF pseudocolour fundus shows multiple (>20) confluent and diffuses not pigmentated BSCR spots irradiating the optic disc, mild papillitis and vitritis. (b) Late-phase UWF fluorescein angiography illustrates leakage at the optic disc with blurriness of margins and papillary vasculature, diffuse leakage of the retinal veins and diffuse capillary leakage (ASUWOG score > 5). (c) UWF indocyanine angiography shows multiple hypofluorescents dark dots consistent with BSCR lesions at mid-phase. (d) Macular oedema is seen in B-scan macular OCT. Compared to an inactive patient with no vitritis, no BSCR spots (e) and normal angiography (f) and indocyanine angiography (g) with no macular oedema (h).

Qualitative assessment of the superficial capillary plexus was performed with the 3 × 3 mm OCT-A frame centred on the foveola (fundus field). There were no differences between groups regarding the presence of telangiectasias, increased intercapillary spaces and capillary irregularity. Conversely, the presence of capillary loops in the active group was significantly higher, with seven eyes (23.3%) versus one (3.3%) in the inactive group ($p = 0.028$; Figure 3c). Therefore, observing vascular loops in the superficial capillary plexus could be a good marker of inflammation activity (Figure 4).

Superficial vascular density and perfusion index, measured via Angioplex® OCT-A in a 6 × 6 mm frame, revealed no significant differences in any of the studied subfields (fundus, superonasal, and inferonasal fields). However, higher vascular density and perfusion index were systematically observed in the active group as compared to inactive. In particular, in the external ETDRS grid ring at the inferonasal field, tended towards significance (A = 19.18 ± 11.15 vs. 14.54 ± 9.03, $p = 0.087$) (Figure 3e,f). As for FAZ there were no differences in area, perimeter or circularity between the two groups (Table 3).

Spearman's correlation matrix showed a significant positive correlation between UWF-FA score and macular volume, nasal retinal thickness, ATRI and subfoveal choroidal thickness, whereas it was significantly negative with AARI. Interestingly, we also observed a significant positive correlation between the inferonasal external perfusion index and the central macular thickness, macular volume and subfoveal choroidal thickness, whereas it was significantly negative with AARI. Therefore, based on the fluorescein angiography score, the higher the score, the higher the macular volume, nasal retinal thickness and ATRI. On the other hand, the higher the macular thickness and volume, the higher the choroidal thickness and the inferonasal perfusion index (Figure 5).

Finally, a multivariate PLS-DA analysis, combining a principal components analysis and logistic regression,

TABLE 1 Classification criteria by clinical and angio-tomographic characteristics at inclusion of active and inactive BSCR eyes.

	Active		Inactive		*p*-Value
n Patients	19	100.0	19	100.0	
n Eyes	30	100.0	30	100.0	
Age (mean/SD)	58.23	12.87	61.23	11.33	0.346
Evolution time (m, mean/SD)	94.73	49.09	127.00	78.23	0.074
Gender–Female (*n*/%)	13	43,3	15	50	0.617
BCVA (LogMAR) (mean/SD)	0.35	0.59	0.28	0.40	0.578
	n	**%**	***n***	**%**	
Previous treatment					
CS intravitreal (*n*/%)	12	40.0	8	26.7	0.291
CS intravitreal/Evolution (*n*)	0.87	1.36	0.60	1.20	0.427
Cumulated PDN (mg) (mean/SD)	1734.50	2402.73	640.00	685.87	**0.011**
Treatment at inclusion					
CS intravitreal	0	0,0	3	10,0	0.119
Systemic CS	11	36.7	3	10.0	**0.018**
Classic synthetic IMT	5	16.7	1	3.3	0.109
Biotherapy	8	26.7	8	26.7	1.000
Inflammation—Vitreous haze (NEI)					
0+	23	76.7	29	96.7	**0.028**
0.5+ to 1+	7	23.3	1	3.3	**0.028**
UWF imaging					
FA score					
≤5	9	30.0	19	63.3	**0.012**
>5	21	70.0	11	36.7	**0.012**
FA score (mean/SD)	9.53	5.63	5.03	4.31	**0.002**
n Spots					
≤3	5	16.7	13	43.3	**0.029**
4–20	21	70.0	6	20.0	**<0.001**
>20	4	13,3	11	36.7	**0.043**
Spot size					
Small	11	36.7	11	36.7	1.000
Medium	12	40.0	5	16.7	0.052
Confluent	7	23.3	14	46.7	0.066
Spot location					
YuxtaPapillary	7	23.3	12	40.0	0.181
Equator	9	30.0	5	16.7	0.243
Diffuse	14	46.7	13	43.3	0.802
Pigmentation					
Absent	24	80.0	21	70.0	0.392
Moderate	6	20.0	6	20.0	1.000
Severe	0	0.0	3	10.0	0.119
Macular cube OCT	Mean	SD	Mean	SD	
CMT	269.53	71.41	222.13	38.71	**0.002**
IR cystic spaces	8	26.7	2	6.7	**0.046**
Macular volume	10.72	1.00	8.97	0.90	**<0.0001**

Note: Significant *p*-values marked in bold.

Abbreviations: BCVA, best-corrected visual acuity; CS, corticosteroids; CMT, central macular thickness; FA, fluorescein angiography; IMT, immunomodulatory therapy; IR, intraretinal; PDN, prednisone; UWF, ultra-wide field.

was implemented to identify discriminant variables between clinically active and inactive BSCR disease. We found that eyes with higher macular volume, ATRI, or thicker nasal retinal thickness, as well as those presenting capillary loops on OCT-A, among others, are independently prone to be clinically active. Perfusion index was the only OCT-A parameter significantly related to active BSCR eyes at the external ring of the inferonasal

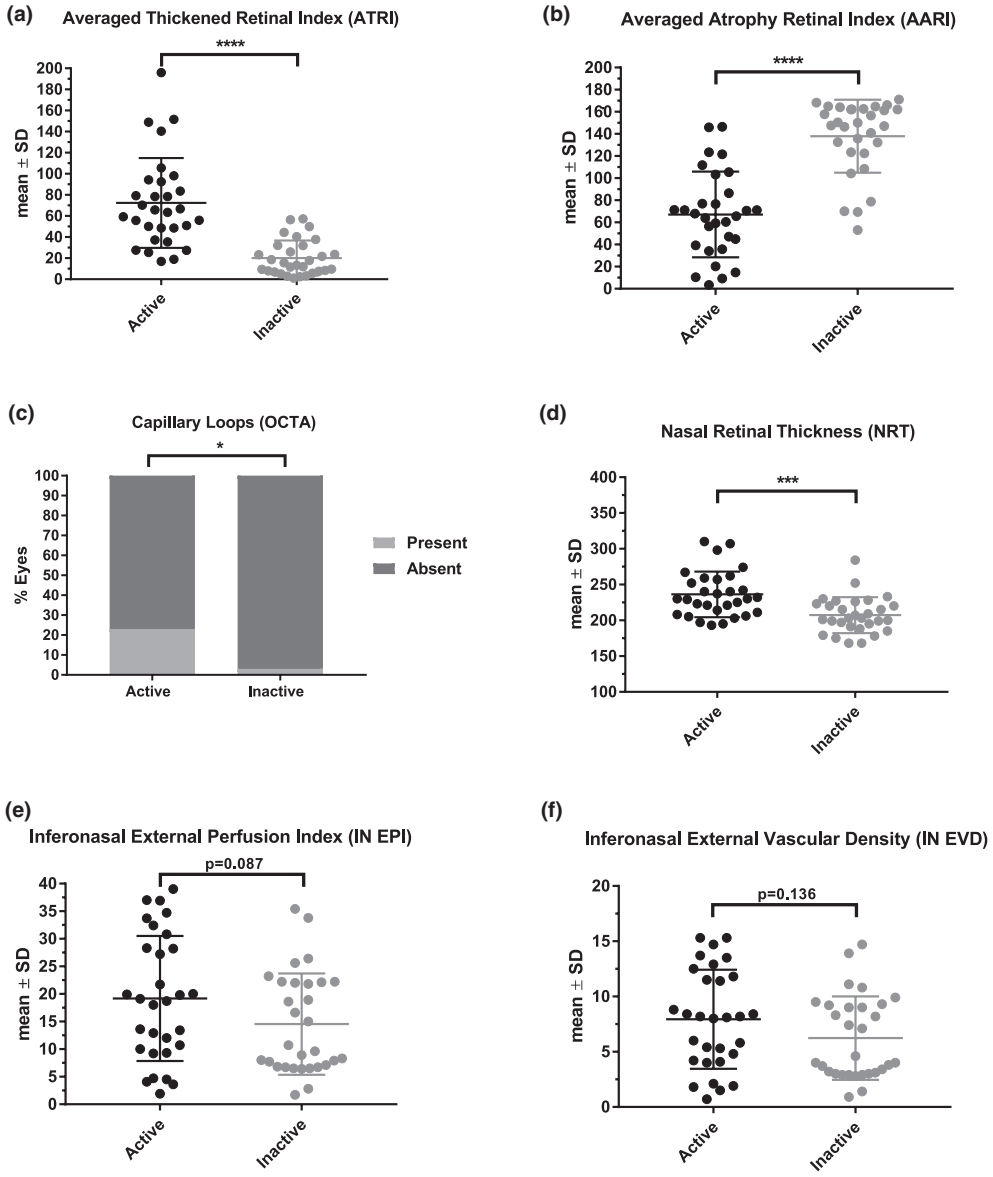

FIGURE 3 Potential biomarkers of BSCR disease activity. Active eyes showed a significantly higher ATRI ($p<0.0001$), lower AARI ($p<0.0001$), presence of vascular loops in the superficial capillary plexus ($p=0.028$) and a higher NRT ($p<0.001$). In the external ETDRS grid ring at the inferonasal area, the perfusion index and vascular density tends to be lower in the inactive group, not reaching statistical significance.

subfield, but with a very low standardized coefficient (Figure 6).

4 | DISCUSSION

BSCR disease is a therapeutically complicated-to-manage disease as its close monitoring is difficult due to the underlying inflammation that these patients may present (Molins et al., 2016). Currently, there is no non-invasive, feasible, quantitative and objective test available that evaluates the disease as a whole and discriminates whether the patient is active or inactive in the short term, to establish or modify treatment.

Currently, we know that the disease evolution time plays a very important role in the prognosis of many BSCR patients since persistent intraocular inflammation leads towards chorioretinal atrophy and disruption of the ellipsoid layer. There is no clear evidence on how and when systemic immunomodulation interrupts the natural history of the disease. On the other hand, there are around 10%–20% of self-limited BSCR that, probably, do not need immunomodulation. Therefore, to monitor BSCR inflammation activity would be very helpful in preventing irreversible damage. However, studies regarding sensitive tests to closely detect BSCR activity are scarce (Bousquet et al., 2022; Gasch et al., 1999; Lages et al., 2019).

In our BSCR groups, active eyes did not require a higher number of intravitreal injections per eye/evolution time, nor longer immunomodulatory or biological treatment/evolution time. This finding supports the idea that there are different BSCR phenotypes, with different natural histories and, consequently, treatment requirements (Lages et al., 2019). Besides a higher systemic cumulated corticosteroid dose in patients with active eyes, our findings suggest a probable immunomodulation-infratreated progressing disease over time in some eyes as some systemic inflammation mediators remain elevated in some apparently inactive patients (Molins et al., 2016).

TABLE 2 Structural tomographic parameters at fundus and nasal fields between active and inactive BSCR eyes.

	Active		Inactive		*p*-Value
n Patients	19	100.0	19	100.0	
n Eyes	30	100.0	30	100.0	
Macular cube OCT	Mean	SD	Mean	SD	
ATRI	72.36	41.88	20.12	16.33	**<0.0001**
AARI	67.15	38.11	137.89	32.49	**<0.0001**
Inferonasal field cube OCT	Mean	SD	Mean	SD	
Nasal retinal thickness (NRT)	236.27	31.36	207.27	24.74	**<0.0001**
Nasal volume	7.53	1.51	6.99	0.95	0.068
EDI-HD B-scan submacular	*n*	%	*n*	%	
Epiretinal membrane	21	70.0	13	43.3	**0.043**
Choroidal thickness (CT)	Mean	SD	Mean	SD	
Total CT	308.27	72.12	257.06	114.59	0.076
Central CT	314.73	75.83	260.90	114.76	0.066
Temporal CT	308.07	69.67	256.27	113.39	0.050
Nasal CT	302.00	76.73	254.00	117.84	0.072
EDI-HD B-scan inferonasal field					
Ellipsoid	*n*	%	*n*	%	
Normal	11	36.7	5	16.7	0.091
Damaged	16	53.3	22	73.3	0.120
Absent	3	10.0	3	10.0	1.000
Choroidal Thickness (CT)	Mean	SD	Mean	SD	
Central CT	212.00	68.37	193.67	71.35	0.318

Note: Significant *p*-values marked in bold.
Abbreviations: AARI, Average Atrophy Retinal Index; ATRI, Average Thickened Retinal Index.

Nevertheless, treatment in patients with inflammatory activity should be more aggressive than in those with no inflammation as has been proposed by the treatment algorithm for the management of BSCR. In fact, inactive patients should be only monitored with no medication (Bousquet et al., 2022).

Clinically, active BSCR showed spots predominantly of medium size and number between 4 and 20 and did not present hyperpigmentation, contrasting with inactive eyes. Patients presenting more than 20 BSCR spots that are confluent and of moderate pigmentation were commonly classified as inactive. Monnet et al. (2006) postulated that greater pigmentation could be the only useful marker of disease progression and, maybe, of decreased visual function. So, the presence of a hyperpigmented fundus could be too late to reverse chorioretinal and functional damage.

In this work, we found an increased perfusion index in active BSCR eyes, which was particularly pronounced in the inferonasal field, as compared to inactive BSCR eyes. Furthermore, the presence of perifoveal capillary looping and an increased ATRI were identified as potential non-invasive biomarkers for close monitoring of BSCR activity.

Structural macular OCT is an excellent non-invasive method to detect and monitor macular oedema. It should be part of the useful tools in the daily clinical practice of these patients. In this study, macular oedema was the most common complication and the greatest cause of central visual loss in these BSCR patients. As expected, it was significantly more frequent in the active group, along with significantly higher central macular thickness and macular volume. Priem et al., in their series including 102 eyes, detected cystoid macular oedema in 63% of cases, and Rothova et al., found it in 84% of 37 patients at some point during a 5-year follow-up (Priem & Oosterhuis, 1988; Rothova et al., 2004).

Our study revealed that ATRI and inferonasal retinal thickness were significantly higher in active eyes. This was consistent with BSCR typical spots' location, radiating from the optic nerve and predominating in the nasal subfields.

Choroidal thickness, both submacular and in the nasal subfield, was found non-significantly lower in inactive than in active patients. Conversely, an accelerated thinning of the choroid via OCT in clinically inactive BSCR patients versus controls with a 3-year follow-up have been described (Young et al., 2015). In the same line, other studies demonstrated a significant subfoveal choroidal thinning and vascular pattern loss with time (Garcia-Garcia et al., 2017; Keane et al., 2013). Altogether, those findings suggest that choroidal thickening is not a sensitive biomarker of current activity, but choroidal thinning over time could be indicative of progression, even in presumed inactive eyes.

We did not find significant changes in the nasal ellipsoid layer in our study; however, Keane et al. (2013), who studied extramacular retinal regions of BSCR patients via EDI-OCT, observed extensive ellipsoid layer disruptions and thinning and loss of the retinal architecture outside the macula, compared with healthy controls. In our patients, the macular ellipsoid layer

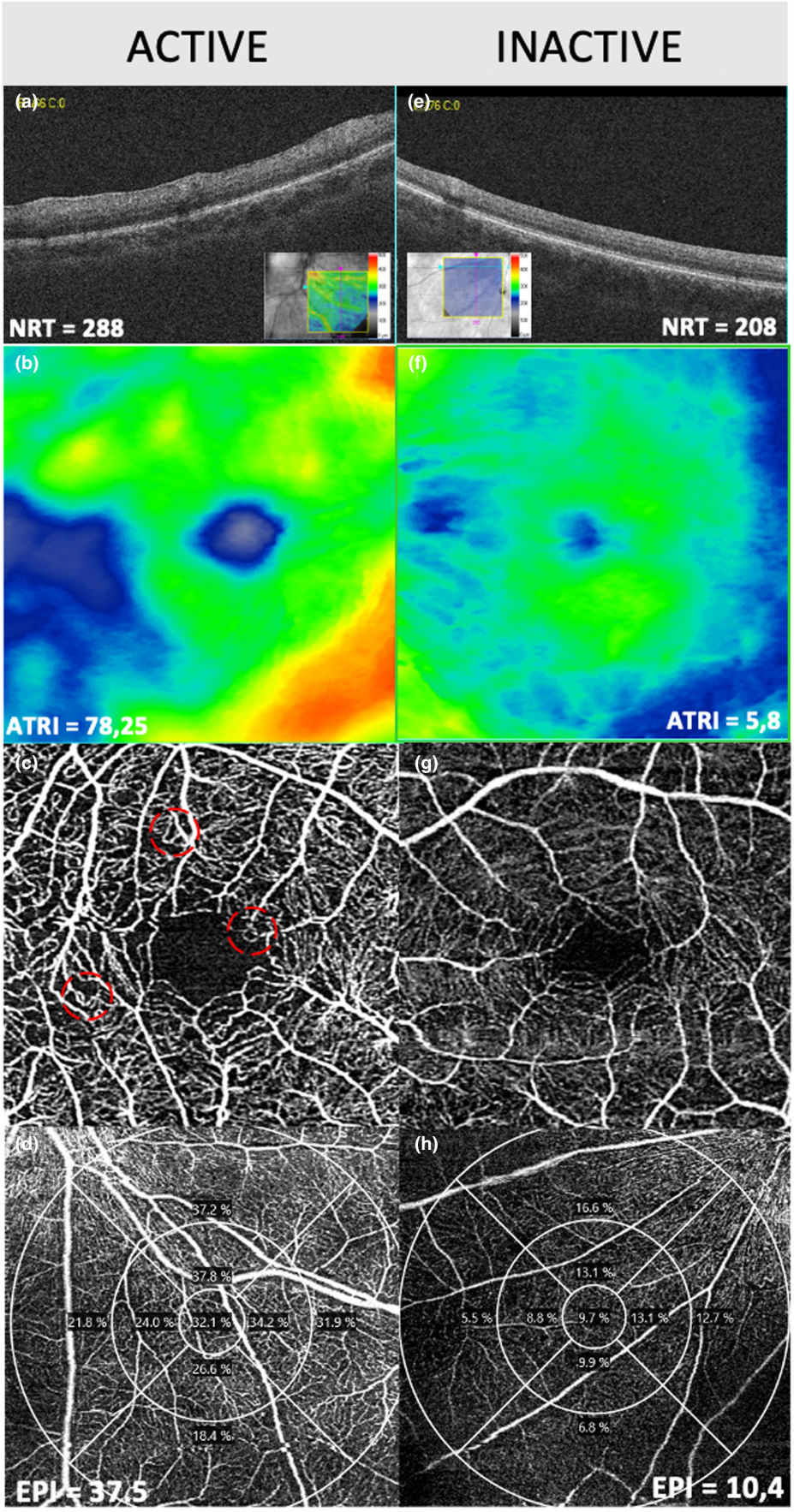

FIGURE 4 Illustrative examples of active (left column) and inactive (right column) BSCR eyes. (a) Higher nasal retinal thickness (NRT), (b) higher averaged thickened retinal index (ATRI), (c) vascular loops are seen in 3 × 3 OCT-A (dashed red circles), (d) higher Inferonasal perfusion index of the external ring (EPI) were found in active BSCR, as compared to inactive eyes (e–h).

TABLE 3 Optic coherence tomography angiography (OCT-A) parameters in BSCR.

	Active		Inactive		*p*-Value
n Eyes	30	100.0	30	100.0	
Fundus field OCTA					
Foveal avascular zone (FAZ)	Mean	SD	Mean	SD	
Area	0.35	0.39	0.36	0.20	0.844
Perimeter	2.67	2.11	2.68	0.73	0.992
Circularity	1.01	2.10	0.61	0.12	0.306
Qualitative assessment	*n*	%	*n*	%	
Telangiectasia	22	73.3	24	80.0	0.561
Increased IC spaces	25	83.3	27	90.0	0.480
Capillary irregularity	22	73.3	22	73.3	1.000
Capillary loops	7	23.3	1	3.3	**0.028**
Fundus field OCTA	Mean	SD	Mean	SD	
Vascular density (VD)					
Total VD	14.48	2.63	13.73	3.66	0.367
Central VD	6.83	3.44	5.54	3.73	0.173
Internal VD	14.07	3.27	13.28	3.98	0.412
External VD	14.90	2.52	14.12	3.64	0.342
Perfusion Index (PI)					
Total PI	34.88	6.97	32.74	9.47	0.328
Central PI	15.16	8.04	12.22	8.40	0.177
Internal PI	33.46	8.29	31.46	10.15	0.408
External PI	36.05	6.80	33.91	9.55	0.325
Superonasal field OCTA	Mean	SD	Mean	SD	
Vascular density (VD)					
Total VD	8.79	4.79	8.30	5.08	0.703
Central VD	7.46	5.66	7.00	5.96	0.760
Internal VD	8.40	5.12	8.07	5.52	0.816
External VD	8.97	4.71	8.42	5.02	0.667
Perfusion Index (PI)					
Total PI	21.52	12.13	20.17	12.81	0.680
Central PI	17.80	13.61	16.65	14.49	0.754
Internal PI	20.60	12.70	19.69	13.83	0.793
External PI	21.96	12.06	20.47	12.66	0.646
Inferonasal field OCTA	Mean	SD	Mean	SD	
Vascular density (VD)					
Total VD	7.72	4.45	6.06	3.69	0.127
Central VD	6.48	5.04	5.27	4.07	0.314
Internal VD	7.23	4.74	5.59	3.87	0.152
External VD	7.94	4.41	6.23	3.71	0.115
Perfusion Index (PI)					
Total PI	18.67	11.21	16.08	16.00	0.472
Central PI	15.74	12.40	12.51	9.85	0.273
Internal PI	17.62	11.94	13.27	9.52	0.130
External PI	19.18	11.15	14.54	9.03	0.087

Note: Comparison between active and inactive eyes at different subfields. Significant *p*-values marked in bold.
Abbreviations: OCTA, optic coherence tomography angiography; PI, Perfusion Index; VD, vascular density.

was damaged or absent, especially in inactive BSCR, however, this difference was not statistically significant. In line with our results, the literature reports that the disruption of this layer is related to a long disease course rather than being an activity marker (Teussink et al., 2016). These authors described disruptions in the ellipsoid zone on OCT in 33% of 42 BSCR eyes and found a good spatial correspondence between this and areas of evident hyperautofluorescent lesions; nevertheless, this hyperautofluorescence pattern did not vary significantly with the activity of the disease (Teussink et al., 2016).

	FAS	CMT	MV	NRT	ATRI	AARI	IN EPI	CO CT
FAS		0.158	0.341	0.347	0.259	-0.304	-0.073	0.263
CMT	0.158		0.653	0.502	0.394	-0.627	0.391	0.264
MV	0.341	0.653		0.734	0.766	-0.892	0.401	0.304
NRT	0.347	0.502	0.734		0.567	-0.697	0.224	0.261
ATRI	0.259	0.394	0.766	0.567		-0.852	0.166	0.128
AARI	-0.304	-0.627	-0.892	-0.697	-0.852		-0.365	-0.174
IN EPI	-0.073	0.391	0.401	0.224	0.166	-0.365		0.267
CO CT	0.263	0.264	0.304	0.261	0.128	-0.174	0.267	

p<0.0001 p<0.001 p<0.01 p<0.05 ns

FAS: fluorescein angiography score, CMT: central macular thickness, MV: macular volume, NRT: nasal retinal thickness, ATRI: averaged thickened retinal index, AARI: averaged atrophy retinal index, IN EPI: inferonasal external perfusion index, CO CT: complete choroidal thickness

FIGURE 5 Correlation matrix (Spearman's). The higher the ATRI, the greater the macular volume and NRT and the lower the AARI. Note that inferonasal perfusion index positively correlates with macular thickness and volume and with choroidal thickness.

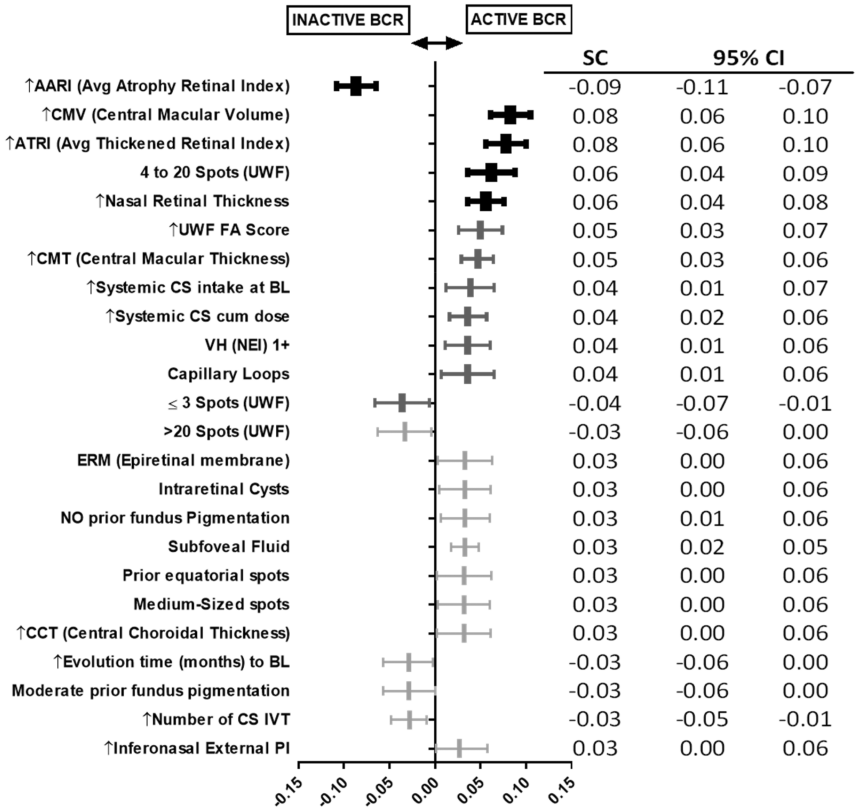

↑ means increased units. UWF: ultra-wide field, Cum: cumulated dose, VH: vitreous haze, BL: baseline, CS: corticosteroids, IVT: intravitreal

FIGURE 6 Multivariate analysis (PLS-DA). Discriminative power of clinical and angio-tomographic variables to BSCR disease activity. All showed covariates are $p<0.05$.

Part of our protocol was to capture extramacular OCT-As in the nasal subfields, both superior and inferior to the optic disc. No quantitative variable (vascular density and perfusion index) at the fundus or nasal fields was significantly different between active and inactive groups. However, there was a general trend towards lower vascular density and perfusion index in all ETDRS grid sectors and, overall, in inactive eyes. Perfusion index in the inferonasal external ring was significantly discriminant in the multivariate analysis, but its power to discern between active and inactive eyes was low. Interestingly, we found a significant positive correlation between the

macular volume and the inferonasal perfusion index. Thus, despite a clear trend to higher retinal perfusion in actively inflamed eyes, this biomarker does not seem sensitive enough to pick up current inflammation activity. The literature, however, reported a decrease in superficial capillary plexus, deep capillary plexus and full retinal vascular density at the macular level in BSCR patients ($n=37$, Optovue®) compared with healthy ones, suggesting that microvascular inflammation and subsequent capillary closure are present thought the retinal vasculature (Roberts et al., 2018). In the absence of age, sex and ethnic standardized reference values for healthy subjects, we also found a slightly lower vascular density and perfusion index in active BSCR eyes than those reported in healthy eyes by some authors at the fundus field (Isik et al., 2021; Polascik et al., 2020). The hypothesis of progressive retinal capillary network closure due to uncontrolled inflammation and subsequent retinal atrophy is supported by those findings.

On the other hand, in line with other reports, no significant changes were detected at the FAZ level between the two groups (Roberts et al., 2018). Conversely, 3 × 3 OCT-A analysis revealed that vascular loops were significantly more frequent in the perifoveal superficial capillary plexus of active eyes, and therefore their presence could be a biomarker of activity. Like us, the groups of Carlo and Pohlman described vascular loops in the superficial plexus in 88% and 58% of BSCR eyes, respectively (De Carlo et al., 2015; Pohlmann et al., 2017). Also, a positive correlation between these microvasculature alterations and longer disease duration was described (Pohlmann et al., 2017). However, we did not find any relationship with evolved eyes but with currently active eyes, which presented more frequent perifoveal capillary looping than inactive eyes, with a similar evolution time from diagnosis in our study.

Retinal vasculitis, predominantly with periphlebitis, peripheral and mid-peripheral capillaritis, optic disc leakage, and macular oedema are typical FA findings in BSCR. We found a fair to moderate positive correlation between FA score and several structural OCT biomarkers of increased retinal thickness in the fundus (macular volume, ATRI) and nasal subfields (nasal retinal thickness). Active eyes showed significantly higher ATRI which strongly correlated with macular volume, nasal retinal thickness and with FA score. Similarly, Knickelbein et al. also found a good positive correlation between the OCT perivascular thickness map and FA in other retinal vasculitis. Among others, Thomas et al., found that greater perivascular thickening was significantly associated with increased retinal vascular leakage on FA, central subfield thickness and total macular volume on OCT in BSCR patients (Knickelbein et al., 2018; Thomas et al., 2019). Moreover, a FA contiguous perineural retinal vascular leakage pattern has been described as more prevalent among BSCR patients than in other non-infectious posterior uveitis and/or primary retinal vasculitis patients, with a positive predictive value of 82.2% (Li et al., 2022). However, most of the findings described were measured manually, in a more restrictive and subjective manner.

An important limitation of this cross-sectional study was the inclusion of some, mostly active, eyes with intraretinal macular cysts and mild vitreous haze, which could skew the quantification of vascular density and perfusion index on OCT-A. Interestingly, despite these limitations, we could find a clear trend towards higher vascular density and perfusion, not only in the fundus, but more pronounced in the inferonasal subfield of active eyes as compared to inactive.

In conclusion, vascular density and perfusion index are diminished in inactive BSCR, particularly in the inferonasal field, however these parameters showed a low discriminative power to discern activity. On the other hand, presence of perifoveal capillary loops on OCT-A and thickening of several fundus retinal structures, which can be objectively quantified by ATRI, along with other clinical signs, could be useful as potential non-invasive biomarker tools for the correct close monitoring of BSCR inflammation activity. A prospective study of changes in these imaging markers after intervention and further external validations are warranted.

ACKNOWLEDGEMENTS

The authors have nothing to report.

ORCID

Aina Moll-Udina https://orcid.org/0000-0003-4753-2111
Marina Dotti-Boada https://orcid.org/0000-0002-8444-2927
Lucía Miguel https://orcid.org/0000-0002-2230-5898
Maite Sainz de la Maza https://orcid.org/0000-0001-8685-766X
Alfredo Manuel Adán Civera https://orcid.org/0000-0002-0849-8814
Blanca Molins https://orcid.org/0000-0003-0941-9134
Victor Llorenç https://orcid.org/0000-0002-7375-1564

REFERENCES

Arya, B., Westcott, M., Robson, A.G., Holder, G.E. & Pavesio, C. (2015) Pointwise linear regression analysis of serial Humphrey visual fields and a correlation with electroretinography in birdshot chorioretinopathy. *The British Journal of Ophthalmology*, 99, 973–978.

Böni, C., Thorne, J.E., Spaide, R.F., Ostheimer, T.A., Sarraf, D., Levinson, R.D. et al. (2017) Fundus autofluorescence findings in eyes with birdshot chorioretinitis. *Investigative Ophthalmology and Visual Science*, 58, 4015–4025.

Bousquet, E., Duraffour, P., Debillon, L., Somisetty, S., Monnet, D. & Brézin, A.P. (2022) Birdshot Chorioretinopathy: a review. *Journal of Clinical Medicine*, 11, 1–17.

Cao, J.H., Silpa-Archa, S., Freitas-Neto, C.A. & Foster, C.S. (2016) Birdshot chorioretinitis lesions on indocyanine green angiography as an indicator of disease activity. *Retina*, 36, 1751–1757.

de Carlo, T.E., Bonini Filho, M.A., Adhi, M. & Duker, J.S. (2015) Retinal and choroidal vasculature in birdshot chorioretinopathy analyzed using spectral domain optical coherence tomography angiography. *Retina*, 35, 2392–2399.

Fich, M. & Rosenberg, T. (1992) Birdshot retinochoroidopathy in monozygotic twins. *Acta Ophthalmologica*, 70, 693–697.

Garcia-Garcia, O., Jordan-Cumplido, S., Subira-Gonzalez, O., Garcia-Bru, P., Arias, L. & Caminal-Mitjana, J.M. (2017) Feasibility of swept-source OCT for active birdshot chorioretinopathy. *Graefe's Archive for Clinical and Experimental Ophthalmology*, 255, 1493–1502.

Gasch, A.T., Smith, J.A. & Whitcup, S.M. (1999) Birdshot retinochoroidopathy. *The British Journal of Ophthalmology*, 83, 241–249.

Isik, M.U., Akay, F., Akmaz, B., Guven, Y.Z. & Isik, I.G. (2021) Normative data of superficial retinal vascular plexus and its relationship with retinal layers. *Beyoglu Eye Journal*, 6, 37–42.

Jabs, D.A., Nussenblatt, R.B., Rosenbaum, J.T. & Standardization of Uveitis Nomenclature (SUN) Working Group. (2005) Standardization of uveitis nomenclature for reporting clinical data. Results of the first international workshop. *American Journal of Ophthalmology*, 140, 509–516.

Keane, P.A., Allie, M., Turner, S.J., Southworth, H.S., Sadda, S.R., Murray, P.I. et al. (2013) Characterization of birdshot chorioretinopathy using extramacular enhanced depth optical coherence tomography. *JAMA Ophthalmology*, 131, 341–350.

Knecht, P.B., Papadia, M. & Herbort, C.P. (2014) Early and sustained treatment modifies the phenotype of birdshot retinochoroiditis. *International Ophthalmology*, 34, 563–574.

Knickelbein, J.E., Tucker, W., Kodati, S., Akanda, M. & Sen, H.N. (2018) Non-invasive method of monitoring retinal vasculitis in patients with birdshot chorioretinopathy using optical coherence tomography. *The British Journal of Ophthalmology*, 102, 815–820.

Kuiper, J.J.W., van Setten, J., Ripke, S., van't Slot, R., Mulder, F., Missotten, T. et al. (2014) A genome-wide association study identifies a functional ERAP2 haplotype associated with birdshot chorioretinopathy. *Human Molecular Genetics*, 23, 6081–6087.

Lages, V., Skvortsova, N., Jeannin, B., Gasc, A. & Herbort, C.P. (2019) Low-grade "benign" birdshot retinochoroiditis: prevalence and characteristics. *International Ophthalmology*, 39, 2111–2120.

Levinson, R.D., Brezin, A., Rothova, A., Accorinti, M. & Holland, G.N. (2006) Research criteria for the diagnosis of birdshot chorioretinopathy: results of an international consensus conference. *American Journal of Ophthalmology*, 141, 185–187.

Li, A., Apivatthakakul, A., Papaliodis, G.N. & Sobrin, L. (2022) High positive predictive value of fluorescein angiography contiguous, perineural retinal vascular leakage pattern for birdshot chorioretinopathy. *Ocular Immunology and Inflammation*, 00, 1–6.

Llorenç, V., Serrano, A.R., Mesquida, M., Lin, P., Esquinas, C., Sainz-de-la-Maza, M. et al. (2021) Swept-source optical coherence tomography objective composite activity score for uveitis. *Acta Ophthalmologica*, 99, 756–764.

Molins, B., Mesquida, M., Llorenç, V., Sainz de la Maza, M. & Adán, A. (2016) Elevated serum immune mediators and subclinical inflammation in HLA-A29-associated birdshot chorioretinopathy. *Ocular Immunology and Inflammation*, 24(6), 647–652.

Monnet, D., Brézin, A.P., Holland, G.N., Yu, F., Mahr, A., Gordon, L.K. et al. (2006) Longitudinal cohort study of patients with birdshot chorioretinopathy. I. Baseline Clinical Characteristics. *American Journal of Ophthalmology*, 141, 135–142.

Nussenblatt, R.B., Mittal, K.K., Ryan, S., Green, W.R. & Maumenee, A.E. (1982) Birdshot retinochoroidopathy associated with HLA-A29 antigen and immune responsiveness to retinal s-antigen. *American Journal of Ophthalmology*, 94, 147–158.

Nussenblatt, R.B., Palestine, A.G., Chan, C.C. & Roberge, F. (1985) Standardizatlon of Vitreal inflammatory activity in intermediate and posterior uveitis. *Ophthalmology*, 92, 467–471.

Pagnoux, C., Mahr, A., Aouba, A., Bérezné, A., Monnet, D., Cohen, P. et al. (2010) Extraocular manifestations of birdshot chorioretinopathy in 118 French patients. *Presse Médicale*, 39, e97–e102.

Pohlmann, D., Macedo, S., Stübiger, N., Pleyer, U., Joussen, A.M. & Winterhalter, S. (2017) Multimodal imaging in birdshot retinochoroiditis. *Ocular Immunology and Inflammation*, 25, 621–632.

Polascik, B.W., Thompson, A.C., Yoon, S.P., Powers, J.H., Burke, J.R., Grewal, D.S. et al. (2020) Association of OCT angiography parameters with age in cognitively healthy older adults. *Ophthalmic Surgery, Lasers & Imaging Retina*, 51, 706–714.

Priem, H.A. & Oosterhuis, J.A. (1988) Birdshot chorioretinopathy: clinical characteristics and evolution. *The British Journal of Ophthalmology*, 72, 646–659.

Roberts, P.K., Nesper, P.L., Goldstein, D.A. & Fawzi, A.A. (2018) Retinal capillary density in patients with birdshot chorioretinopathy. *Retina*, 38, 387–394.

Rothova, A., Berendschot, T.T.J.M., Probst, K. & Benson, W.E. (2004) Birdshot chorioretinopathy: long-term manifestations and visual prognosis. *Evidence-Based Eye Care.*, 111, 954–959.

Shah, K.H., Levinson, R.D., Yu, F., Goldhardt, R., Gordon, L.K., Gonzales, C.R. et al. (2005) Birdshot chorioretinopathy. *Survey of Ophthalmology*, 50, 519–541.

Sobrin, L., Lam, B.L., Liu, M., Feuer, W.J. & Davis, J.L. (2005) Electroretinographic monitoring in birdshot chorioretinopathy. *American Journal of Ophthalmology*, 140, 52.e1–52.e18.

Standardization of Uveitis Nomenclature (SUN) Working Group. (2021) Classification criteria for birdshot Chorioretinitis. *American Journal of Ophthalmology*, 228, 65–71.

Teussink, M.M., Huis in het Veld, P.I., de Lam, V., Hoyng, C.B., Klevering, B.J. & Theelen, T. (2016) Multimodal imaging of the disease progression of birdshot chorioretinopathy. *Acta Ophthalmologica*, 94, 815–823.

Thomas, A.S., Hatef, A.L., Stinnett, S.S., Keenan, R.T. & Jaffe, G.J. (2019) Perivascular thickening on optical coherence tomography as a marker of inflammation in birdshot retinochoroiditis. *Retina*, 39, 956–963.

Thorne, J.E., Jabs, D.A., Kedhar, S.R., Peters, G.B. & Dunn, J.P. (2008) Loss of visual field among patients with birdshot chorioretinopathy. *American Journal of Ophthalmology*, 145, 23–28.e2.

Tugal-Tutkun, I., Herbort, C.P., Khairallah, M. & Angiography Scoring for Uveitis Working Group (ASUWOG). (2010) Scoring of dual fluorescein and ICG inflammatory angiographic signs for the grading of posterior segment inflammation (dual fluorescein and ICG angiographic scoring system for uveitis). *International Ophthalmology*, 30, 539–552.

Young, M., Fallah, N. & Forooghian, F. (2015) Choroidal degeneration in birdshot chorioretinopathy. *Retina*, 35, 798–802.

Zacks, D.N., Samson, C.M., Loewenstein, J. & Foster, C.S. (2002) Electroretinograms as an indicator of disease activity in birdshot retinochoroidopathy. *Graefe's Archive for Clinical and Experimental Ophthalmology*, 240, 601–607.

How to cite this article: Moll-Udina, A., Dotti-Boada, M., Miguel, L., Rodríguez, A., Gascón, J., Sainz de la Maza, M. et al. (2023) Non-invasive biomarkers for close activity monitoring in birdshot chorioretinitis: Optical coherence tomography angiography and beyond. *Acta Ophthalmologica*, 00, 1–12. Available from: https://doi.org/10.1111/aos.15744